

Toxoplasma gondii Arginine Methyltransferase 1 (PRMT1) Is Necessary for Centrosome Dynamics during Tachyzoite Cell Division

Kamal El Bissati,^{a*} Elena S. Suvorova,^b Hui Xiao,^c Olivier Lucas,^b Rajendra Upadhy,^{a*} Yanfen Ma,^a Ruth Hogue Angeletti,^c Michael W. White,^b Louis M. Weiss,^{a,d} Kami Kim^{a,d,e}

Department of Pathology, Albert Einstein College of Medicine, Bronx, New York, USA^a; Department of Molecular Medicine, USF Health College of Medicine, University of South Florida, Tampa, Florida, USA^b; Laboratory for Macromolecular Analysis and Proteomics, Albert Einstein College of Medicine, Bronx, New York, USA^c; Department of Medicine, Albert Einstein College of Medicine, Bronx, New York, USA^d; Department of Microbiology and Immunology, Albert Einstein College of Medicine, Bronx, New York, USA^e

* Present address: Kamal El Bissati, Department of Surgery, The University of Chicago, Chicago, Illinois, USA; Rajendra Upadhy, Department of Molecular Microbiology, Washington University School of Medicine, St. Louis, Missouri, USA.

ABSTRACT The arginine methyltransferase family (PRMT) has been implicated in a variety of cellular processes, including signal transduction, epigenetic regulation, and DNA repair pathways. PRMT1 is thought to be responsible for the majority of PRMT activity in *Toxoplasma gondii*, but its exact function is unknown. To further define the biological function of the PRMT family, we generated *T. gondii* mutants lacking PRMT1 ($\Delta prmt1$) by deletion of the *PRMT1* gene. $\Delta prmt1$ parasites exhibit morphological defects during cell division and grow slowly, and this phenotype reverses in the $\Delta prmt1::PRMT1mRFP$ complemented strain. Tagged PRMT1 localizes primarily in the cytoplasm with enrichment at the pericentriolar material, and the strain lacking PRMT1 is unable to segregate progeny accurately. Unlike wild-type and complemented parasites, $\Delta prmt1$ parasites have abnormal daughter buds, perturbed centrosome stoichiometry, and loss of synchronous replication. Whole-genome expression profiling demonstrated differences in expression of cell-cycle-regulated genes in the $\Delta prmt1$ strain relative to the complemented $\Delta prmt1::PRMT1mRFP$ and parental wild-type strains, but these changes do not correlate with a specific block in cell cycle. Although PRMT1's primary biological function was previously proposed to be methylation of histones, our studies suggest that PRMT1 plays an important role within the centrosome to ensure the proper replication of the parasite.

IMPORTANCE Apicomplexan parasites include several important pathogens, including *Toxoplasma gondii*, a major cause of opportunistic infections and congenital birth defects. These parasites divide using a unique form of cell division called endodyogeny that is different from those of most eukaryotes. PRMT1 is a conserved arginine methyltransferase that was thought to regulate gene expression of *T. gondii* by modifying histone methylation. Using genetic techniques, we show that disruption of PRMT1 affects the parasite's ability to perform accurate cell division. Our studies reveal an unexpected role for arginine methylation in centrosome biology and regulation of parasite replication.

Received 3 December 2015 Accepted 31 December 2015 Published 2 February 2016

Citation El Bissati K, Suvorova ES, Xiao H, Lucas O, Upadhy R, Ma Y, Hogue Angeletti R, White MW, Weiss LM, Kim K. 2016. *Toxoplasma gondii* arginine methyltransferase 1 (PRMT1) is necessary for centrosome dynamics during tachyzoite cell division. mBio 7(1):e02094-15. doi:10.1128/mBio.02094-15.

Invited Editor John C. Boothroyd, Stanford University **Editor** L. David Sibley, Washington University School of Medicine

Copyright © 2016 El Bissati et al. This is an open-access article distributed under the terms of the [Creative Commons Attribution-Noncommercial-ShareAlike 3.0 Unported license](https://creativecommons.org/licenses/by-nc-sa/4.0/), which permits unrestricted noncommercial use, distribution, and reproduction in any medium, provided the original author and source are credited.

Address correspondence to Louis M. Weiss, louis.weiss@einstein.yu.edu, or Kami Kim, kami.kim@einstein.yu.edu.

This article is a direct contribution from a Fellow of the American Academy of Microbiology.

Toxoplasma gondii, a member of the phylum Apicomplexa, is an obligate intracellular parasite and an important human pathogen. Because it can be transmitted by food and water *T. gondii* is a category B biodefense priority pathogen. The parasite is widespread in its host range and geographical distribution, with an age-adjusted prevalence of 12.9% in the United States in 2009 to 2010 (1). *T. gondii* can differentiate from the rapidly replicating tachyzoite stage into a latent cyst form, the bradyzoite stage. Differentiation between parasite life cycle stages is accompanied by significant alterations in the expressed transcriptome, as well as remodeling of *T. gondii* chromatin structure, a major mechanism by which the access to genomic DNA is restricted and regulated. Histone modifications in the Apicomplexa are proposed to act in concert with other putative epigenetic information carriers (his-

tone variants and small RNAs) and ApiAP2 DNA sequence-specific transcription factors (2) to trigger the recruitment of the transcriptional machinery to specific genes. Methylation of arginine and lysine residues in histones can modulate gene expression positively or negatively (3), and both arginine and lysine methyltransferases are proposed to be important regulators of gene expression in *T. gondii* (4).

An extensive repertoire of arginine methylation machinery is present in *T. gondii* compared with yeast and *Caenorhabditis elegans* (5). Bioinformatic analysis of the *Toxoplasma* genome sequence (<http://www.toxodb.org>) demonstrates five putative arginine methyltransferases (5) that are expressed in *T. gondii* based upon mRNA studies (<http://www.toxodb.org>). The primary structure of each PRMT shares a conserved methyltransferase do-

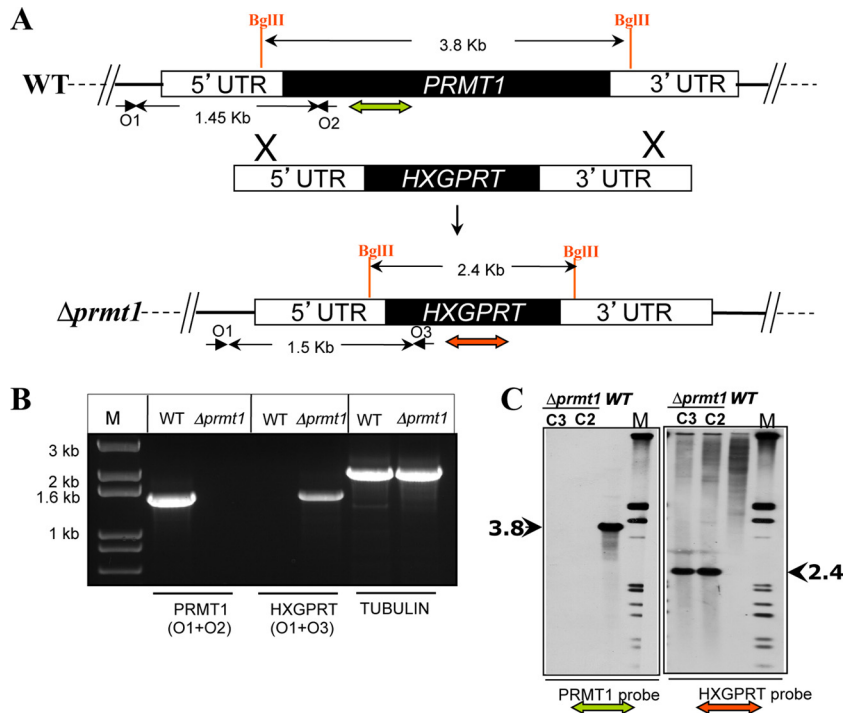


FIG 1 Disruption of the *PRMT1* locus. (A) Strategy for *PRMT1* disruption by double crossover. (Top) A schematic representation of the native *PRMT1* chromosomal locus is shown. (Middle) One kilobase of untranscribed region (UTR) flanking the *PRMT1* gene coding region was used for induction of the homologous recombination for stable transformation of *T. gondii*. (Bottom) Proposed model of integration of the plasmid by double crossover into the *PRMT1* chromosomal locus. (B) PCR analysis of the *PRMT1* chromosomal locus in the wild-type strain (WT) and $\Delta prmt1$ strain (clone 2). Using primers (O1, O2, and O3) described in Materials and Methods and denoted by the arrows in panel A, the wild-type (1.45 kb) and disrupted *PRMT1* (1.5 kb) loci were confirmed by PCR. (C) Southern analysis of the *PRMT1* locus in wild-type (WT) and $\Delta prmt1$ parasites (clones 2 and 3, labeled C2 and C3, respectively). Integration at the *PRMT1* locus was verified by Southern analysis using probes to the *PRMT1* ORF or to HXGPRT, probe locations are indicated by the red and green double-headed arrows in panel A (No BglII site was found on the endogenous HXGPRT gene).

main that includes subdomains for binding to the methyl donor, *S*-adenosyl-L-methionine (SAM) and substrate proteins. PRMTs have a broad spectrum of substrates, including RNA-processing proteins, RNA-transporting proteins, protein phosphatase 2A, G proteins, and histones (6) but relatively little is known about PRMTs in *T. gondii*. PRMT1 (TGME49_219520) has been reported to mediate methylation of arginine 3 of H4 and PRMT4 (TgCARM1) to mediate the methylation of arginine 17 of H3 (5). The families of methyltransferases and demethylases is expanded in *T. gondii* (4, 7), suggesting protein methylation may have an expanded role in the biology of *T. gondii* with roles unrelated to histone modification. In support of this conjecture, recent studies have demonstrated methylation of *T. gondii* apical cytoskeletal proteins mediated by AKMT1 (8) as well as methylation of tubulin mediated by an unidentified methyltransferase (9).

To address the function of arginine methyltransferases on gene expression of *T. gondii*, mutants lacking *PRMT1* were created by double-targeted gene replacement within the virulent type I strain RH using a strategy employing linear fragments to disrupt the gene (10). Parasites lacking PRMT1 harbor morphological defects during cell division and grow slower than the wild-type (WT) parental strain due to an inability to accurately count the number of daughter cells and segregate nuclear material. This defect is reversed in the complemented (Cm) mutant. Although differences in histone methylation and gene expression are evident in the $\Delta prmt1$ strain, our genetic studies indicate the most important

function of PRMT1 is in regulation of daughter cell counting required for proper cell division.

RESULTS

Generation of *PRMT1* knockout strain and restoration by complementation. To evaluate the importance of *PRMT1* in parasite differentiation, transgenic parasites lacking *PRMT1* (*PRMT1* knockout [KO]) were generated. A targeting vector with 1 kb flanking the *PRMT1* gene was constructed using the Gateway system (Fig. 1A) (10). Transfection of RH parasites with the linear fragment followed by selection on mycophenolic acid with xanthine resulted in double-crossover homologous recombination with loss of the entire *PRMT1* open reading frame (ORF). Diagnostic PCR analysis with various combinations of primer pairs demonstrated the integration of the hypoxanthine-xanthine-guanine-phosphoribosyl transferase (HXGPRT) cassette into the *PRMT1* locus and the absence of intact *PRMT1* (Fig. 1B). Southern blot analyses on genomic DNA using various probes specific for *PRMT1* or HXGPRT further confirmed disruption of the *PRMT1* chromosomal locus by a double-crossover event in two separate independent clones tested (Fig. 1C). Both $\Delta prmt1$ strains were complemented with a cassette encoding a PRMT1-mCherry fusion protein (PRMT1mRFP) driven by the heterologous *TUB1* promoter. *PRMT1* expression in the $\Delta prmt1::PRMT1mRFP$ strain was confirmed by reverse transcriptase PCR (see Fig. S1A in the supplemental material), immunoblot analysis (see Fig. S1B), and

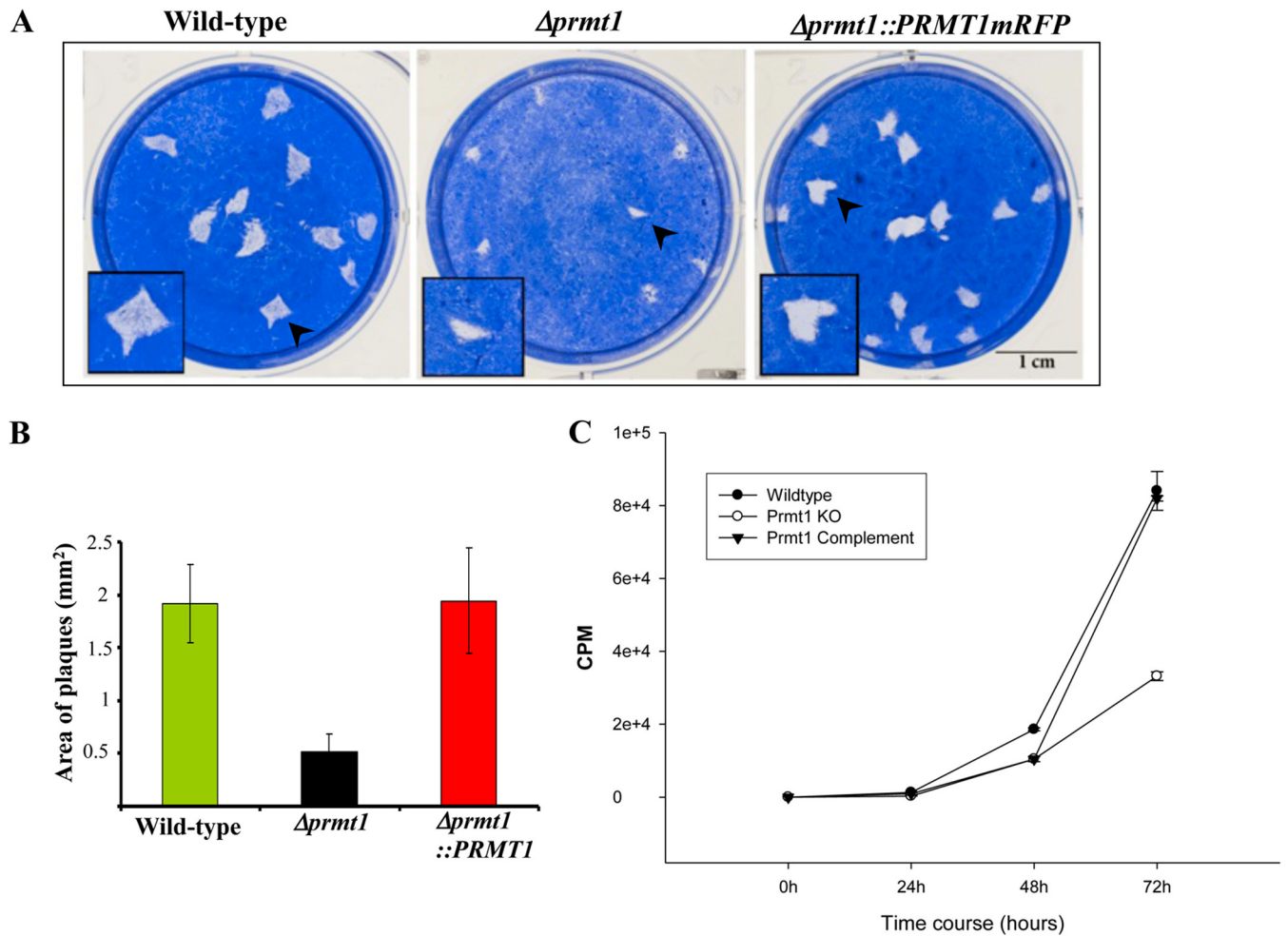


FIG 2 *PRMT1* knockout parasites display growth defects *in vitro*. (A) $\Delta prmt1$ parasites formed plaques significantly smaller than those formed by the parental RH $\Delta hxp1$ (left), and the complemented $\Delta prmt1::PRMT1mRFP$ strains (right). (B) Areas of plaques in cubic millimeters measured using $\Delta prmt1$ and $\Delta prmt1::PRMT1mRFP$ strains versus the wild-type parental line are shown with standard deviations. (C) The defect in plaque size reflects a general defect in intracellular growth, as reflected in uracil incorporation assays performed with tachyzoites grown in pH 7 media. Uracil incorporation determined in triplicate with standard deviations is shown. A low inoculum (100 parasites) was chosen so that it did not lyse the monolayer at 48 h.

fluorescence microscopy (see Fig. S1C). PRMT1mRFP was evident throughout the cell, including the nucleus, but has a predominantly cytosolic distribution (see Fig. S1C).

Knockout of *PRMT1* results in an *in vitro* growth defect in *Toxoplasma* tachyzoites. To assess the importance of PRMT1 for growth of the tachyzoites, we performed plaque assays and found that growth of the $\Delta prmt1$ parasites was significantly impaired. Although the numbers of plaques were comparable between analyzed strains, the $\Delta prmt1$ parasites formed an average of 3- to 4-times-smaller plaques than those formed by the parental and complemented strains $\Delta prmt1::PRMT1mRFP$ (Fig. 2A and B). The ability to develop normal plaques depends not only on the replication rate but also on the invasion, efficient egress, and motility of the extracellular parasites (11). Neither egress nor motility was affected by the depletion of PRMT1 (see Fig. S2 in the supplemental material), suggesting that impaired replication of the intracellular tachyzoites was likely responsible for reduced plaque size. Consistent with these findings, the $\Delta prmt1$ parasites showed reduced uracil incorporation compared to the complemented $\Delta prmt1::PRMT1mRFP$ strain and wild-type cells (Fig. 2C).

To determine if the $\Delta prmt1$ mutant exhibits decreased virulence *in vivo*, we infected groups of mice with 10 $\Delta prmt1$, $\Delta prmt1::PRMT1mRFP$, or wild-type parental tachyzoites intraperitoneally. Consistent with their slower replication rate, $\Delta prmt1$ parasites showed a modest delay in time to death when 10 parasites were used to infect mice, with partial complementation in the $\Delta prmt1::PRMT1mRFP$ strain, although all mice in all three groups died (see Fig. S2 in the supplemental material).

$\Delta prmt1$ parasites have modest differences in histone methylation. Previous studies of *Toxoplasma* PRMT1 using an antibody to H4R3me2 demonstrated that recombinant protein (rPRMT1) can methylate a recombinant histone 4 with an arginine but not a lysine at the 3 position (5). To determine if H4R3me modification was present in *T. gondii* tachyzoites, we purified histones H3 and H4 from the wild-type and $\Delta prmt1$ strains (Fig. 3A). Histone methylation was mapped by mass spectrometry techniques. Using this analysis we could not detect methylation of arginine 3 of histone H4 in either wild-type or $\Delta prmt1$ strain (Fig. 3B) (data not shown). Using a more exhaustive mass spectrometry approach to define histone PTM comprehensively, we

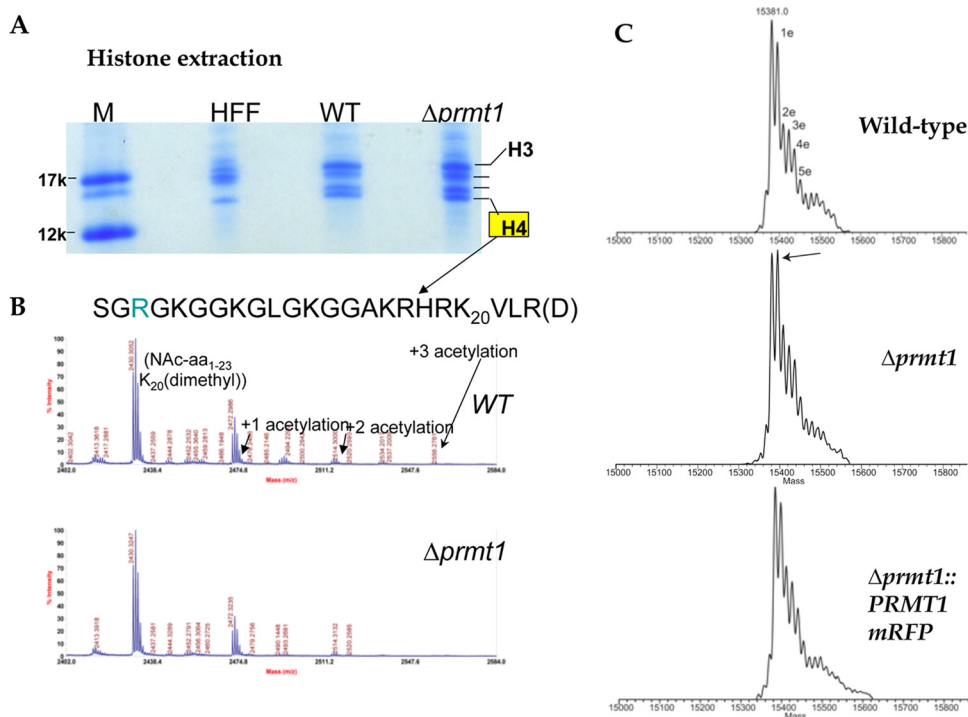


FIG 3 Parasites lacking PRMT1 have increased monomethylation of histone H3. (A) Histones were extracted from HFF host cells, purified RH Δ hxgprt (WT) tachyzoites, and from Δ prmt1 strain tachyzoites by acid extraction and fractionated by SDS-polyacrylamide gel electrophoresis. The Coomassie blue-stained gel is shown with molecular standards. Histone H4 was cut from the gel and digested with Asp-N to release the N-terminal peptide. (B) Deconvoluted electrospray mass spectrum of the N-terminal peptide SGRGKGGKGLGKGGAKRHRK₂₀VLR(D) of gel-extracted *T. gondii* histone 4 from panel A following Asp-N digestion. Neither strain shows evidence of H4R3 methylation. (C) Mass spectrometry of gel-extracted intact H3 from Δ prmt1, Δ prmt1::PRMT1mRFP, and wild-type parasites. The Δ prmt1 strain shows increased monomethylation of H3 (arrow) relative to wild-type parasites, which is reversed in the complemented Δ prmt1::PRMT1mRFP parasites.

have detected H4R3 methylation in a subset of H4R3 peptides, suggesting that this modification is substoichiometric (12). We also examined the global modification profile of histone H3 from wild-type, knockout, and complemented parasites (Fig. 3C). Surprisingly, we found an increase of monomethylation of H3 in the Δ prmt1 parasites that was reversed in the Δ prmt1::PRMT1mRFP line (Fig. 3C). Thus, while differences in histone methylation were evident, deletion of PRMT1 did not result in the expected change in H4R3 methyl modification. In light of these findings, we used cell biology approaches to further define the phenotype of Δ prmt1 parasites, hypothesizing that PRMT1 activity could regulate non-histone substrates in either the cytosol or nucleus.

PRMT1 localizes to the mitotic structures during tachyzoite replication. While performing immunofluorescence assays, we noticed that parasites within Δ prmt1 vacuoles were disorganized and lost the typical symmetric arrangement within vacuoles. This abnormality, visualized by transmission electron microscopy (see Fig. S1D in the supplemental material), suggests that the main phenotypic defect is likely to be during cell division. We performed a detailed characterization of the cell cycle expression of PRMT1 in Δ prmt1::PRMT1mRFP parasites using well-established nuclear and cellular morphological criteria (13, 14). Transgenic parasites were costained with anti-IMC1 (15) to monitor the presence of internal daughters and 4',6-diamidino-2-phenylindole (DAPI) to visualize the nuclei during G₁, late S phase/early mitosis when daughter buds first appear, and during parasite budding and nuclear division. PRMT1mRFP was present throughout the cell

but was highly concentrated in a single proteinaceous cloud localized to the apical side of the nucleus in G₁ parasites (Fig. 4). In late-S-phase parasites (S/M), this structure is duplicated and then is associated with daughter buds during mitosis and cytokinesis (M/C). Thus, PRMT1 was enriched in the apical region with cytoskeletal structures involved in cell division.

PRMT1mRFP-associated structures were further defined using cell cycle comarkers MORN1-myc2x (16) and ISP1 (17) (Fig. 5). PRMT1mRFP was encircled with the MORN1 ring structures (Fig. 5A), a localization that corresponds to the position of the centrosome (14). In Δ prmt1::PRMT1mRFP parasites costained with MORN1-myc2x and ISP1, an early marker of daughter bud formation (17) (Fig. 5B), PRMT1mRFP localized to a structure that lies underneath the apical cone of the bud and becomes fully separated from the early bud structures. Finally, staining with anti-human centrin1 antibody placed centrioles in the middle of PRMT1mRFP focal accumulation, similar to the recently described pericentriolar material (PCM) factor *T. gondii* mitogen-activated protein kinase-L1 (TgMAPK-L1) (18). Thus, based on the cell cycle dynamics of PRMT1mRFP and colocalization with specific mitotic markers, we conclude that PRMT1mRFP is localized to the centrosome and the pericentrosomal PCM compartment (Fig. 5C).

The eukaryotic centrosome is a hub that coordinates multiple events during cell division. Because *Toxoplasma* division is unusually complex, particularly at the phase of mitosis coupled to cytokinesis, these parasites evolved a bipartite centrosome that allows

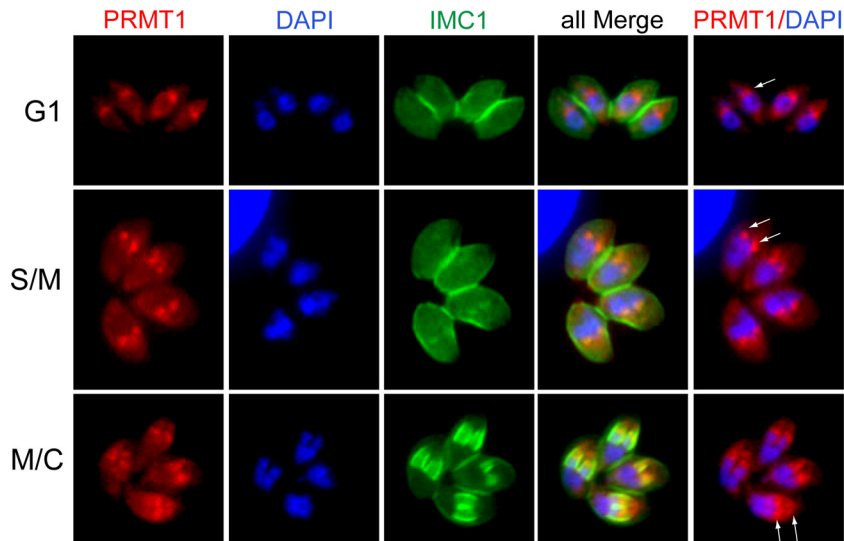


FIG 4 PRMT1 is associated with mitotic structures during tachyzoite replication. Cell cycle expression of PRMT1 in $\Delta prmt1::PRMT1mRFP$ parasites was monitored by red native fluorescence. Parasites were costained with anti-IMC1 (green) to indicate parasite size and the presence of internal daughters and DAPI (blue) to visualize nuclear chromosomes. Cell cycle phases were identified by well-established nuclear and cellular morphological criteria. The representative subcellular distribution of PRMT1mRFP is shown in three major cell cycle transitions: in G_1 , in late-S-phase/early mitosis (prophase/first appearance of buds), and during parasite budding and nuclear division (telophase/cytokinesis). Note that PRMT1mRFP is concentrated in a single structure localized to the apical side of the nucleus in G_1 parasites (white arrow in the PRMT1-DAPI merged image, top panel). In late-S-phase parasites (S/M), this structure is duplicated and is associated with daughter buds during mitosis and cytokinesis (M/C).

segregation of centrosomal functions (18). Deficiency of the PCM kinase TgMAPK-L1 affects coordination of karyokinesis and cytokinesis, which manifests as unregulated amplification of the centrin cores and delayed budding. Similarly, deletion of *PRMT1* is associated with multinuclear replication with irregular centrosome counts (Fig. 6). The centrosome duplication observed in wild-type and complemented $\Delta prmt1::PRMT1mRFP$ parasites that had entered S phase was accurate and synchronous with the expected even numbers of parasites (Fig. 4 to 6). In contrast, centrosome numbers were nonstoichiometric and replicated asynchronously in $\Delta prmt1$ parasites (Fig. 6A). Irregular centrosome numbers in the $\Delta prmt1$ parasites were enumerated and confirmed the observed replication defect (Fig. 6B). We also observed a pronounced defect of karyokinesis, including DNA missegregation and formation of zoites, which implicates an effect of PRMT1 deficiency upon the DNA segregation machinery.

Differential gene expression for *prmt1*Δ knockout. To further assess the role of PRMT1 in gene expression of *T. gondii* and to identify genes that might have altered expression in response to the absence of PRMT1, we performed whole-genome expression profiling to compare the wild-type, $\Delta prmt1$, and complemented $\Delta prmt1::PRMT1mRFP$ strains. Affymetrix ToxoGeneChip microarrays, which contain probe sets for ~8,000 predicted *Toxoplasma* genes, were used for this study (19). The differentially regulated genes were grouped into functional categories based on Gene Ontology (GO) annotations in the *Toxoplasma* genome database at www.toxodb.org. The data set of differentially expressed transcripts for the three strains is available in Data Set S1 in the supplemental material.

PRMT1 signal was present in the wild-type strain, depleted in the $\Delta prmt1$ mutant, and overexpressed in the complemented line, validating the disruption of *PRMT1* by microarray analysis. Although we anticipated that differences in gene expression would

reflect a cell cycle block, both G_1 and S/M genes were dysregulated (Fig. 7), and the pattern of altered expression did not suggest a perturbation of the periodicity of the cell cycle expressed in tachyzoites unique to the $\Delta prmt1$ strain (versus wild-type and complemented lines), as determined by comparison of differentially regulated genes (Fig. 7) or by using gene set enrichment analysis (GSEA) (20; data not shown). When we compared the 58 genes that were differentially expressed in both wild-type and complemented strains relative to the knockout strain, several cytoskeletal genes potentially important for cell segregation were dysregulated, including the genes coding for MORN1, γ -tubulin, axonemal dynein heavy chain, and a striated fiber assemblin (SFA1) (Fig. 7; see Data Set S1 in the supplemental material). γ -Tubulin, along with α -tubulin and β -tubulin, is found in centrosomes and spindle pole bodies. SFA2 and SFA3 tether the centrosome to the daughter cell microtubule organizing center (MTOC) and are essential for cytokinesis (21). The function of SFA1 has not been defined, but SFA1 could have a function in other stages, including endopolygeny seen in cat gut stages. *Apicomplexa* are unusual in having both the centrosome (a phylogenetically conserved MTOC) and the apical polar ring, an apicomplexan-specific MTOC that is critical for segregation of organelles during daughter formation. *PRMT1* expression may have both direct effects upon the assembly of centrosome proteins required for daughter cell budding as well as indirect effects via expression of genes critical for accurate parasite replication.

DISCUSSION

The arginine methyltransferase family has been implicated in a plethora of cellular processes, including signal transduction, epigenetic regulation, and DNA repair pathways (22, 23). PRMT1 is thought to be responsible for the majority of PRMT activity in yeast (24), trypanosomes (25), and human cells (26). We have

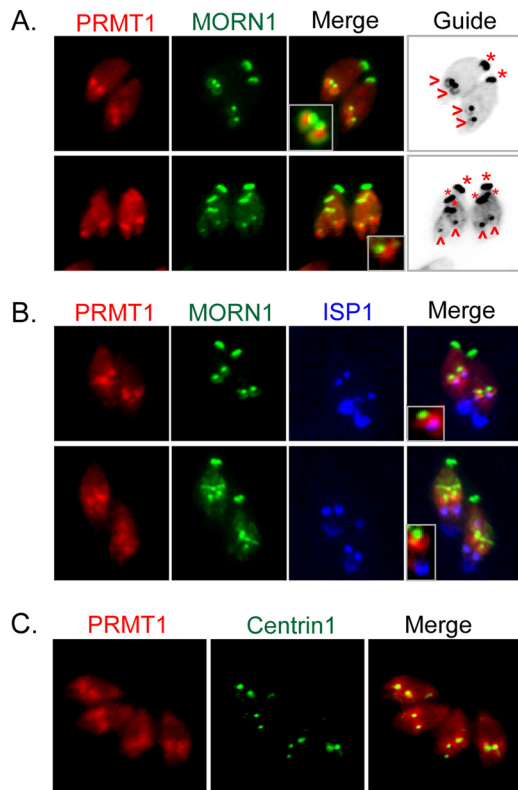


FIG 5 PRMT1 is concentrated in the pericentrosomal compartment. PRMT1mRFP-associated structures were further defined using cell cycle comarkers. (A) Parasite clones expressing PRMT1mRFP ($\Delta prmt1::PRMT1mRFP$ [red, native fluorescence]) were transfected with a plasmid carrying a copy of MORN1-myc2x (green, anti-Myc costaining) (16) and the two proteins visualized during the first 24 h postelectroporation. A marker guide panel, which is a black and white inverse of the MORN1 and anti-IMC1 (not shown individually) combined staining patterns, provides a labeled reference of the MORN1-associated spindle pole with rings (>) and the mother cell basal complex (*). Note that PRMT1mRFP is inside the center of the MORN1 ring structures (see inset images, red stain), which is the location of the centrosome during this stage of the parasite cell cycle (14). (B) To further resolve PRMT1-associated structures, $\Delta prmt1::PRMT1mRFP$ parasites (red), were costained for MORN1-myc2x (green) and ISP1 (blue), which is an early marker of daughter bud formation (17). The color resolution in these images (see inset panels) indicates PRMT1mRFP localizes to a structure that lies underneath and becomes fully separated from the early bud structures (e.g., blue versus red in inset images in the bottom panel). (C) Staining with anti-human-centrin1 (green, centrosomes) shows PRMT1mRFP colocalizes to this structure and the pericentriolar compartment that surrounds the organelle.

investigated the function of PRMT1, a methyltransferase whose orthologues are found in the cytoplasm and the nucleus of both yeast and human cells (27–29). Expression of the *PRMT1* gene is not required for cell viability in yeast and mammals (26, 27, 30). Nevertheless, PRMT1 is essential during development as mice with reduced PRMT1 expression die during embryogenesis (26). PRMT1 also plays an important role in the *Trypanosoma brucei* life cycle, where depletion of PRMT1 expression via RNA interference results in growth impairment and nuclear defects in the bloodstream forms (31) but not in procyclic forms of the parasite (25).

PRMT1 in yeast and in humans is primarily a nuclear protein, whereas *T. gondii* PRMT1 is primarily cytoplasmic, providing a first hint that perhaps PRMT1 has different functions in this par-

asite. *Toxoplasma* is unique among apicomplexan parasites in possessing five arginine methyltransferases (PRMT1 to -5) compared to three PRMTs in yeast, *C. elegans*, and *Plasmodium* (32). Saksoouk et al., using a polyclonal antibody to H4R3me2 and an *in vitro* assay with recombinant histone H4, suggested that PRMT1 methylates arginine 3 of histone 4 in *T. gondii* (5). They therefore hypothesized that PRMT1 functions in gene regulation as histone-modifying enzymes, but the importance of PRMT1 was not tested.

We sought to delineate the role of PRMT1 by making genetic knockouts in type I RH strain parasites. Our knockout strategy involved transfection with a linear Gateway fragment to knock out the *PRMT1* gene (10). The loss of *PRMT1* was accompanied by morphological defects during cell division and slow growth of the parasite. A $\Delta prmt1::PRMT1mRFP$ complemented strain no longer exhibited the growth defect observed in the $\Delta prmt1$ strain, proving the defect was due to deletion of *PRMT1* rather than off-target effects. $\Delta prmt1$ mutants have a defect in replication that results in abnormal vacuoles, but the effect on virulence in mice was modest in the highly virulent RH genetic background. The steady-state mRNAs for all five arginine methyltransferases in the genome are cell cycle regulated (33) with similar peak expression, and it is possible that any role that *PRMT1* plays in gene regulation is partially functionally redundant with the activities of the other PRMT or that PRMT1 plays a more important role in strains that are less laboratory adapted than RH.

Surprisingly, we observed increased monomethylation of H3 in the $\Delta prmt1$ strain that was reversed upon complementation of PRMT1. This phenomenon has also been reported in mammals, where disruption of PRMT1, the major PRMT, alters the accessibility of substrates leading to paradoxically increased methylation (34). There were no differences in steady-state mRNA of the other 4 PRMTs detectable in microarray analysis, suggesting that the altered methylation was unlikely to be due to compensatory increased expression of the other PRMTs. Thus, there appears to be a complex interplay between the different enzymes involved in methylation of *T. gondii* proteins, and further experimentation will be required to dissect the direct versus indirect effects of PRMT1 activity.

In other organisms, PRMT1 is thought to regulate gene expression by methylating histones and nuclear factors important for transcription or by modifying the activity of RNA binding proteins. Gene expression profiling demonstrated significant alteration of mRNA expression of $\Delta prmt1$ strain genes, many of which were cell cycle regulated; however, there was not a significant difference in S/M gene expression or G₁ gene expression that might point to a specific block or delay in cell cycle, nor were we able to identify gene sets uniquely dysregulated in the $\Delta prmt1$ strain.

Based on analogy to other systems, proteins with a repeating arginine-glycine-glycine (RGG) motif, commonly mRNA-processing proteins, are candidate substrates for PRMT1 (32). Potential candidate substrates include Argonaute 1 (AGO1), an essential component of the RNA-induced silencing complex (RISC) involved in RNA-induced silencing activities in both the nucleus and cytoplasm (35). PRMT1 was identified in a pulldown of the TgAGO1 complex (35), suggesting that PRMT1 could regulate TgAGO1 assembly within macromolecular complexes, as reported for PRMT5 in *Drosophila melanogaster* (36). TgAGO1 interacts with and is methylated by PRMT1 (37), but regulated depletion of PRMT1 had a more significant effect upon parasite replication than depletion of AGO1 (37), suggesting that the growth pheno-

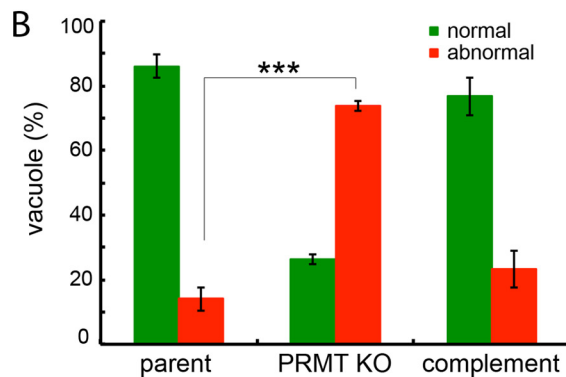
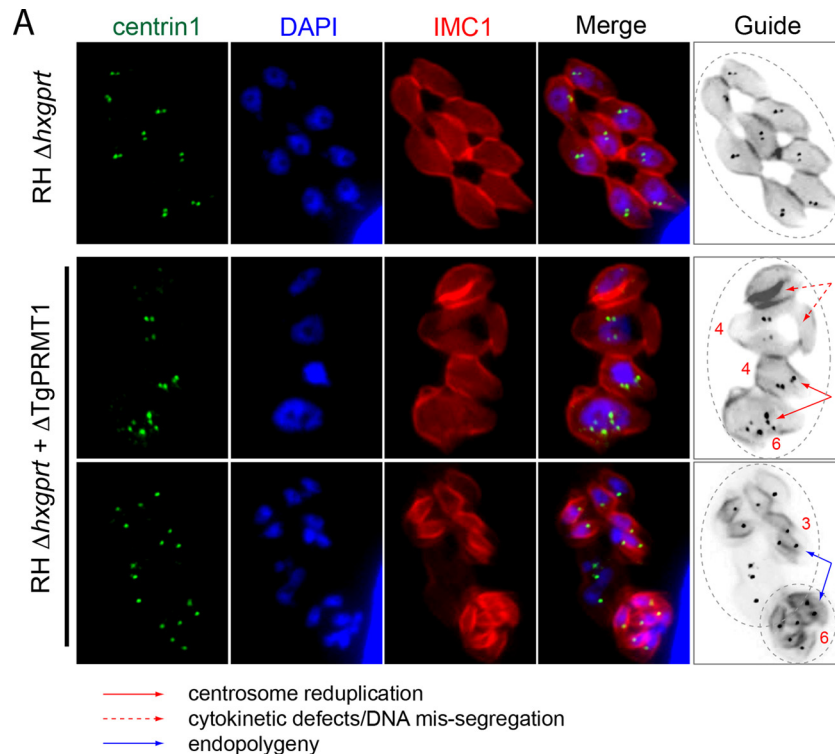


FIG 6 Deletion of *PRMT1* leads to abnormal parasite counting. (A) *Toxoplasma* centrosomes have a strict stoichiometric relationship in cell division, with duplication of the centrosome preceding the formation of two daughters in each tachyzoite cell cycle. Centrosome duplication observed in parasites that had entered S phase (green, anti-human centrin1) was accurate and synchronous in the eight parental parasites that shared the same vacuole (top panel). In contrast, centrosome numbers were nonstoichiometric and asynchronously replicated in $\Delta prmt1$ parasites lacking the *PRMT1* gene (bottom two panels). Irregular centrosome numbers in the knockout parasites are enumerated in the guide reference panels. Three phenotypic features are associated with deletion of *PRMT1*: (i) daughter buds are abnormal (dashed red arrows), (ii) centrosome counts exceed stoichiometric numbers (solid red arrows), and (iii) multinuclear replication is associated with irregular centrosome counts reminiscent of endopolygeny (blue arrows). All of these features were considered abnormal in the quantification below. The costains in these images were anti-IMC1 (red), which indicates parasite size and the presence of internal daughters, and DAPI (blue), which was used to visualize nuclear chromosomes. (B) The fraction of normal and abnormal vacuoles was quantified in wild-type parental, $\Delta prmt1$, and $\Delta prmt1::PRMT1mRFP$ parasite clones (100 total vacuoles counted in triplicate per clone). *PRMT1* deletion led to significant increase in the amount of abnormal vacuoles (***, $P < 10^{-6}$).

type seen by depletion of *PRMT1* was not due to perturbation of the genes potentially regulated by AGO1 and the RISC.

Intriguingly, in parasites lacking *PRMT1*, expression of several genes linked to parasite replication was dysregulated. Among these were the genes coding for MORN1, a protein essential for basal body formation and cytokinesis (16, 38, 39), and SFA1, one of three striated fiber assemblins. SFAs are apicomplexan proteins that are homologues of the striated rootlet fiber of algal flagella. SFA2 and SFA3 are cell cycle regulated and play an essential role

formation of a fibrillar tether that couples the daughter microtubule organizing center, a unique apicomplexan apical structure, to the centrosome during mitosis (21). The steady-state transcript of SFA1, a third SFA that is not cell cycle regulated and is not highly expressed, is induced in the knockout, as is the mRNA of γ -tubulin. γ -Tubulin is required for microtubule nucleation and is found in centrosomes and spindle body poles. Induction of γ -tubulin and SFA mRNA in the *PRMT1* knockout could contribute to dysregulation or impaired formation of daughter buds. In

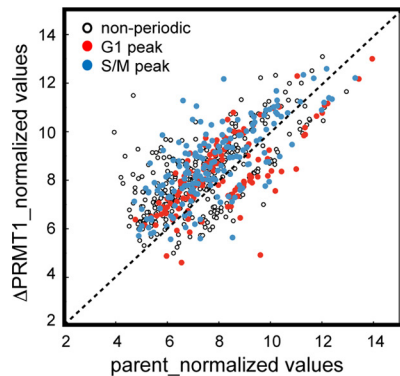


FIG 7 Dysregulation of gene expression in the *PRMT1* knockout is not cell cycle specific. Total RNA (three independent biological samples per strain) from asynchronously grown parent and $\Delta prmt1$ strains was obtained, converted to cRNA, and used to hybridize Affymetrix *Toxoplasma* GeneChips. Published mRNAs from the cell cycle transcriptome with peak expression in the G₁ versus S/M periods were evaluated in the parent and $\Delta prmt1$ gene expression profiles. Significant values (normalized RMA values) with more than a 2-fold change were identified and compared (see parent versus $\Delta prmt1$ mutant in the graph on the left). Genes with increased mRNA expression in the $\Delta prmt1$ strain were plotted above the dashed line, while declining mRNA levels in comparison to those of the parent cells were plotted below. Note that both G₁ (red) and S/M (blue), transcripts were affected in the $\Delta prmt1$ strain, indicating the growth phenotype of this strain does not cause a cell cycle timing defect. Consistent with the abnormal structural features seen in $\Delta prmt1$ parasites, the regulation of genes involved in centrosome duplication and cytokinesis was significantly altered compared to that in the parent strains. Selected genes showing at least 2-fold difference in expression in the knockout compared to the wild type are shown in the table to the right. These genes also showed similar expression differences compared to the complemented strain (see Data Set S1 for details).

Description	Genbank	FC KO/WT
arginine N-methyltransferase 1	TGME49_019520	-25.80
MORN repeat-containing protein	TGME49_023060	-5.22
Atypical MEK-related kinase	TGME49_066950	-2.96
axonemal dynein heavy chain	TGME49_061020	-2.22
ankyrin repeat-containing protein	TGME49_016680	-2.10
tubulin gamma chain	TGME49_026870	3.38
SF-assemblin	TGME49_107840	4.86

In addition to these proteins, several other proteins potentially involved in cytoskeletal structure or cell signaling have altered expression in wild-type and the complemented strain compared to the knockout strain (see Data Set S1 in the supplemental material). Many of the proteins with altered expression are hypothetical proteins whose importance has yet to be determined. PRMT1 could methylate histones or other nuclear factors with resultant downstream effects on gene expression or modify cytosolic substrates that affect mRNA levels.

In summary, this study provides genetic evidence for an important role for PRMT1 in *Toxoplasma* replication. PRMT1 localization to the centrosome and pericentriolar material and the significant abnormalities in parasite endodyogeny associated with *PRMT1* deletion indicate that PRMT1 acts to regulate the processes required for accurate daughter cell counting during parasite replication. Several recent studies identified a number of centrosomal proteins implicated in the control of *T. gondii* cell division. In addition to Nek1 (40) and Aurora-related kinase 1 (18), an unusual member of the MAPK family kinases, TgMAPKL-1, was shown to restrict duplication of the centrosome to once per cycle, thus demonstrating secure binary division of the *Toxoplasma* tachyzoite (18). Interestingly, both PRMT1 and MAPKL-1 localize to pericentriolar matrix, and PRMT1 deficiency led to a less devastating but similar loss of control of centrosome duplication. It is tempting to hypothesize that cell division in apicomplexan parasites is regulated not only by phosphorylation of the target proteins with kinases but also by protein methylation with PRMT1. Although methylation of centrosomal proteins has not been described in any eukaryote, in human cells, methylation of Golgi factors by cytoplasmic PRMT5 is critical for the proper organelle assembly and function (41, 42)

Our study suggests that protein arginine methylation regulates parasite replication. In *T. gondii*, PRMT1 is associated with the centrosome throughout the cell cycle, and lack of PRMT1 results in abnormal daughter buds, perturbed centrosome stoichiometry, and loss of synchronous replication. Although PRMT1 functions

are often conserved, PRMT1 substrates cannot be accurately predicted based only upon sequence, and species-specific differences in substrate specificity have been reported (25). Reagents and proteomic approaches have been utilized to survey the methylome of *T. brucei* (43, 44), and similar studies will be useful to elucidate the mechanism by which PRMT1 regulates daughter segregation. *Plasmodium* PRMT1 has similar localization to TgPRMT1 and has also been thought to function in gene regulation (45). It will be of great interest to determine whether PRMT1 has a conserved function in apicomplexan parasite division since blood-stage malaria parasites replicate by schizogony rather than endodyogeny. Further studies to identify PRMT1 substrates may determine how various posttranslational modifications of histone and nonhistone proteins regulate parasite replication and accurate centrosome duplication.

MATERIALS AND METHODS

Parasite culture. *T. gondii* RH $\Delta hxpprt$ tachyzoites were used in all experiments, and the maintenance of parasites by continuous passage in human foreskin fibroblasts (HFFs) and parasite transfections were performed as previously described (46).

Generation of $\Delta prmt1$ and $\Delta prmt1::PRMT1mRFP$. *PRMT1* (TGME49_219520) was cloned from RH strain parasites. One-kilobase fragments upstream of the *PRMT1* initiator codon and downstream of the stop codon were cloned to flank a hypoxanthine-xanthine-guanine-phosphoribosyl transferase (HXGPRT) cassette, transformed into RH $\Delta hxpprt$ parasites, selected with 50 $\mu\text{g}\cdot\text{ml}^{-1}$ xanthine plus 25 $\mu\text{g}\cdot\text{ml}^{-1}$ mycophenolic acid (46), and cloned by limiting dilution as described previously (47). $\Delta prmt1$ parasites were genetically complemented with a construct containing the *TUB1* promoter upstream of the *PRMT1* cDNA with an mCherryFP (mRFP) tag fused to the C terminus. The plasmid ptub-PRMT1-mRFP was constructed by replacing the PRMT1/NheI-BglII fragment in ptub-EGFP-mCherryFP. (The plasmid was a kind gift from Ke Hu, University of Indiana). $\Delta prmt1$ parasites were cotransfected with a plasmid conferring resistance to chloramphenicol. After selection in 10 μM chloramphenicol plus 50 $\mu\text{g}\cdot\text{ml}^{-1}$ xanthine with 25 $\mu\text{g}\cdot\text{ml}^{-1}$ mycophenolic acid, parasites were cloned by limiting dilution and assessed for PRMT1 expression. Since initial phenotypic analysis results

were similar for the two clones, further cell biology and biochemical characterization was performed with one set of knockout and complemented lines. The parental RH Δ hgxprt strain (wild type [WT]), the Δ prmt1 mutant (also referred to as the knockout [KO]), and the Δ prmt1::PRMT1mRFP strain (complemented [Cm]) were compared in the following assays.

Plaque assay. Fully confluent HFFs were infected with equal numbers of parental RH Δ hgxprt, Δ prmt1, and Δ prmt1::PRMT1mRFP parasites for 11 days. The cultures were fixed and permeabilized in cold methanol (-20°C) for 15 min and stained with Coomassie brilliant blue G-250 dye at room temperature for 1 h and then at 4°C overnight before scanning and measuring plaque size.

Uracil incorporation growth assay. [^3H]uracil incorporation was applied to test the growth of the wild-type (RH Δ hgxprt), Δ prmt1, and prmt1::PRMT1mRFP strains (48). Twelve-well tissue culture plates containing confluent HFF monolayers were inoculated with the parasites (1×10^2 /well) for 24, 48, and 72 h in pH 7.1 medium with 5% CO_2 or pH 8.1 medium with 0.5% CO_2 . The inoculum was calculated so that the HFF monolayer was not completely lysed after 48 h and that a 72-h time point could be acquired. Mean values from 3 independent experiments \pm standard deviations are shown.

Static gliding assay. Glass coverslips were coated overnight at 4°C with 50% fetal bovine serum (FBS)–50% phosphate-buffered saline (PBS). Freshly lysed filtered tachyzoites were resuspended in HHE (Hanks balanced salt solution [HBSS], 10 mM HEPES, 1 mM EGTA), and the coated slides were inoculated with 250 μl for 30 min at 37°C . The slides were then fixed with 3% paraformaldehyde. Parasites were also pretreated with the gliding inhibitor cytochalasin D as a negative control or with dimethyl sulfoxide (DMSO [solvent control]). Trails left by gliding parasites were visualized at $40\times$ by staining with the mouse anti-SAG1 antibody followed by a conjugated anti-mouse secondary antibody. Between 40 and 200 trails were enumerated per strain per treatment as previously detailed (49, 50).

Time-lapse video for motility and egress. Infected HFF monolayers were washed in HBSS 24 to 36 h postinfection and exposed to 4 μM A23187 for video microscopy. The image time series were collected at 10-s intervals for up to 20 min and converted to time-lapse video.

Transmission electron microscopy. The carbon-coated Matrigel-covered samples with *Toxoplasma*-infected cells were fixed with 2.5% glutaraldehyde and 0.5% tannic acid in 0.1 M sodium cacodylate buffer, postfixed with 1% osmium tetroxide followed by 2% uranyl acetate, dehydrated through a graded series of ethanol, and embedded in LX112 resin (Ladd Research Industries). Ultrathin sections were cut on an Ultracut UCT (Reichert), stained with uranyl acetate followed by lead citrate, and viewed on a transmission electron microscope (1200EX; JEOL) at 80 kV at the Analytic Imaging Facility of the Albert Einstein College of Medicine.

Western blotting. Parasites were isolated from host cells by two successive passages through a 25-gauge needle and one passage through a 3- μm -pore filter, followed by centrifugation at $500 \times g$ for 10 min. The parasite pellet was washed twice in PBS and lysed in SDS sample buffer. Equal amounts of protein were loaded into wells of a 12% SDS–polyacrylamide gel and fractionated by electrophoresis. The proteins were transferred to nitrocellulose membranes, and immunoblotting was performed with rabbit anti mCherryFP as the primary antibody, revealed with conjugated goat anti-rabbit as the secondary antibody. Signal generation was performed using an ECL enhanced chemiluminescence kit (PerkinElmer Life Sciences).

Immunofluorescence assay analysis. Confluent HFF cultures on glass coverslips were infected with parasites for the indicated times. Cells were fixed in 3.7% paraformaldehyde, permeabilized in 0.25% Triton X-100, and blocked in 1% bovine serum albumin (BSA) in PBS. PRMT1mRFP was detected by native fluorescence after fixation and antibody staining for other comarkers. Epitope-tagged MORN1 protein was visualized after transient transfection with a plasmid carrying a MORN1-

myc2x insert (16). Incubations with primary antibody (1 h) followed by the corresponding secondary antibody (1 h) were performed at room temperature with DAPI (0.5 $\mu\text{g}/\text{ml}$) added in the final incubation to stain genomic DNA. The following primary antibodies were used at the indicated dilutions: mouse monoclonal anti-Myc (MORN1 staining; Santa Cruz Biotechnology, Santa Cruz, CA), anti-ISP1 (early budding structures, monoclonal antibody kindly provided by Peter Bradley, UCLA), and anti-IMC1 (mature buds and mother cell shape; kindly provided by Gary Ward, University of Vermont) at 1:1,000. Serum raised against the conserved human centrin1 (26-14.1; a kind gift from Ian Cheeseman, MIT) was previously shown to cross-react with the *Toxoplasma* centrin orthologue and provide visualization of parasite centrosomes (13, 51). All Alexa-conjugated secondary antibodies (Molecular Probes, Life Technologies) were used at a 1:1,000 dilution. After several washes with PBS, coverslips were mounted with Aquamount (Thermo Scientific), dried overnight at 4°C , and viewed on a Zeiss Axiovert Microscope equipped with a $100\times$ objective. Images were processed in Adobe Photoshop CS v4.0 using linear adjustment for all channels.

Virulence studies. Groups of 4 mice were intraperitoneally injected with 10 tachyzoites and observed for up to 30 days for mortality in 2 separate experiments. The numbers of injected parasites were confirmed by plaque assay and were equivalent between groups. All animal experiments were conducted in AAALAC approved facilities using protocols approved by the Animal Use Committee of the Albert Einstein College of Medicine.

HPLC and mass spectrometric analysis of intact histone samples. For high-performance liquid chromatography (HPLC), histones were purified from tachyzoites using a histone purification kit (Active Motif, Carlsbad, CA). A Shimadzu high-performance liquid chromatograph with two LC-10AD pumps was used to generate a gradient with a 30- $\mu\text{l}/\text{min}$ flow rate. Solvent A was 5% acetonitrile in H_2O with 0.1% fluorescent antibody (FA), while solvent B consisted of 95% acetonitrile in H_2O with 0.1% FA. After desalting for 5 min with 5% B, the histone samples were eluted at 30 $\mu\text{l}/\text{min}$ with a 5 to 50% gradient for 30 min. The effluent was infused into a 12-T Varian IonSpec FT-ICR (Agilent, Inc.) or an LTQ linear ion trap mass spectrometer (Thermo Scientific) for analysis.

Mass spectrometric analysis of in-gel-digested proteolytic histone samples. Histone purification was performed as previously described (52). Histones purified from tachyzoites were resolved by SDS-PAGE, and the gel was stained with Coomassie blue. Bands with individual histones were cut from the gel. After destaining, the gel piece with H4 was incubated for 18 h at 37°C with endoproteinase Asp-N (Roche, Indianapolis, IN) in 50-mM sodium phosphate buffer (pH 8.0). Digested peptides were recovered from the gel by three extractions with 50:50 H_2O –acetonitrile–5% formic acid. The extracted peptides were mixed (1:1) with an α -cyano-4-hydroxycinnamic acid solution (50:50 H_2O –acetonitrile containing 0.1% trifluoroacetic acid [TFA]). A 1- μl aliquot of the mixture was placed on a matrix-assisted laser desorption ionization (MALDI) target and air dried. Mass spectra were acquired on a 4800 MALDI tandem time of flight (TOF/TOF) mass spectrometer (Applied Biosystems, Foster City, CA). The instrument was equipped with an Nd:YAG laser (PowerChip, JDS Uniphase, San Jose, CA) operating at 200 Hz and controlled by Applied Biosystems 4000 series Explorer version 3.6 software. Each spectrum was accumulated in 500 shots. Tandem mass spectra were searched against the EPICDB compiled *T. gondii* database (53) using the MASCOT program (Matrix Sciences, London, United Kingdom).

RNA purification, probe construction, microarray hybridizations, and analysis. *T. gondii* RH Δ hgxprt (wild-type parent), Δ prmt1 (knockout), and Δ prmt1::PRMT1mRFP (complemented) parasites were harvested from each flask by scraping and then isolated from host cells by two successive passages through a 25-gauge needle and one passage through a 3- μm -pore filter. Total RNA was processed using the RNeasy protocol (Qiagen), with mercaptoethanol added to the lysis solution and DNase I treatment performed prior to RNA elution. RNA sample quality was assessed on a model 2100 Bioanalyzer (Agilent Biotechnologies). Synthesis

and fragmentation of cRNA probes followed Affymetrix one-cycle protocols and hybridizations to the *Toxoplasma* GeneChip array (see <http://ancillary.toxodb.org/docs/Array-Tutorial.html> for a description of the array design) was performed on the Affymetrix GeneChip Station following standard methods as previously described (54) at the Montana State University Functional Genomics Core Facility. Three biological replicates were run for each parasite line.

To minimize variations among independent experiments, samples were processed together for probe synthesis and hybridization. For each sample type, three independent RNA samples were harvested for a total of three hybridizations per sample type. Hybridization data were preprocessed with RMA (robust multiarray average), normalized using per chip and per gene median polishing, and analyzed using the software package GeneSpring GX11 (Agilent Technologies, Santa Clara, CA). Probe sets with a raw value greater than 50 under at least 1 out of 9 conditions were retained ($n = 7,038$) for *t* test analysis that further refined the list to 809 probe sets. An analysis of variance (ANOVA) was run to identify genes with significantly greater than random variation in RNA abundance between the wild-type, $\Delta prmt1$, and $\Delta prmt1::PRMT1mRFP$ lines. Variances were calculated with a *P* value cutoff of 0.05 and multiple testing correction (Benjamini and Hochberg) (33). To further filter the gene lists, we identified genes whose expression changed in both $\Delta prmt1$ versus the wild-type parental strain and between the $\Delta prmt1$ and complemented $\Delta prmt1::PRMT1mRFP$ lines. This list was manually inspected. All expression data for genes that had a statistically significant change in expression are shown in Data Set S1 in the supplemental material.

Microarray data accession number. Data have been deposited as an NCBI Geo Dataset under accession number [GSE73177](https://www.ncbi.nlm.nih.gov/geo/query/acc.cgi?acc=GSE73177).

SUPPLEMENTAL MATERIAL

Supplemental material for this article may be found at <http://mbio.asm.org/lookup/suppl/doi:10.1128/mBio.02094-15/-/DCSupplemental>.

Figure S1, TIF file, 0.9 MB.

Figure S2, TIF file, 0.4 MB.

Data Set S1, XLSX file, 0.9 MB.

ACKNOWLEDGMENTS

We are grateful to Rima McLeod for critical reading of the manuscript. We also thank Ke Hu for the TUB1-mCherry vector, and Gary Ward, Peter Bradley, and Ian Cheeseman for antibodies. We also acknowledge the technical assistance of Kate McInerney at the Montana State microarray facility.

This research was supported by National Institutes of Health grants R01AI087625 (K.K.), RC4AI092801 (K.K. and M.W.W.), R01AI095094 (L.M.W.), and R01AI077662 and R01AI089885 (M.W.W.). We also acknowledge the support of the Einstein-Montefiore Center for AIDS Research, funded by P30AI051519.

FUNDING INFORMATION

HHS | National Institutes of Health (NIH) provided funding to Kami Kim under grant numbers R01AI087625, RC4AI092801, and P30AI051519. HHS | National Institutes of Health (NIH) provided funding to Louis M. Weiss under grant number R01AI095094. HHS | National Institutes of Health (NIH) provided funding to Michael W. White under grant numbers R01AI077662, R01AI089885, and RC4AI092801.

P30AI051519 supports the Einstein-Montefiore Center for AIDS Research.

REFERENCES

- Jones JL, Kruszon-Moran D, Rivera HN, Price C, Wilkins PP. 2014. *Toxoplasma gondii* seroprevalence in the United States 2009–2010 and comparison with the past two decades. *Am J Trop Med Hyg* 90: 1135–1139. <http://dx.doi.org/10.4269/ajtmh.14-0013>.
- Balaji S, Babu MM, Iyer LM, Aravind L. 2005. Discovery of the principal specific transcription factors of Apicomplexa and their implication for the evolution of the AP2-integrase DNA binding domains. *Nucleic Acids Res* 33:3994–4006. <http://dx.doi.org/10.1093/nar/gki709>.
- Zhang X, Yang Z, Khan SI, Horton JR, Tamaru H, Selker EU, Cheng X. 2003. Structural basis for the product specificity of histone lysine methyltransferases. *Mol Cell* 12:177–185. [http://dx.doi.org/10.1016/S1097-2765\(03\)00224-7](http://dx.doi.org/10.1016/S1097-2765(03)00224-7).
- Bougdour A, Braun L, Cannella D, Hakimi MA. 2010. Chromatin modifications: implications in the regulation of gene expression in *Toxoplasma gondii*. *Cell Microbiol* 12:413–423. <http://dx.doi.org/10.1111/j.1462-5822.2010.01446.x>.
- Saksouk N, Bhatti MM, Kieffer S, Smith AT, Musset K, Garin J, Sullivan WJ, Jr, Cesbron-Delauw MF, Hakimi MA. 2005. Histone-modifying complexes regulate gene expression pertinent to the differentiation of the protozoan parasite *Toxoplasma gondii*. *Mol Cell Biol* 25: 10301–10314. <http://dx.doi.org/10.1128/MCB.25.23.10301-10314.2005>.
- Aletta JM, Cimato TR, Ettinger MJ. 1998. Protein methylation: a signal event in post-translational modification. *Trends Biochem Sci* 23:89–91. [http://dx.doi.org/10.1016/S0968-0004\(98\)01185-2](http://dx.doi.org/10.1016/S0968-0004(98)01185-2).
- Sullivan WJ, Jr, Hakimi MA. 2006. Histone mediated gene activation in *Toxoplasma gondii*. *Mol Biochem Parasitol* 148:109–116. <http://dx.doi.org/10.1016/j.molbiopara.2006.03.010>.
- Heaslip AT, Nishi M, Stein B, Hu K. 2011. The motility of a human parasite, *Toxoplasma gondii*, is regulated by a novel lysine methyltransferase. *PLoS Pathog* 7:e1002201. <http://dx.doi.org/10.1371/journal.ppat.1002201>.
- Xiao H, El Bissati K, Verdier-Pinard P, Burd B, Zhang H, Kim K, Fiser A, Angeletti RH, Weiss LM. 2010. Post-translational modifications to *Toxoplasma gondii* alpha- and beta-tubulins include novel C-terminal methylation. *J Proteome Res* 9:359–372. <http://dx.doi.org/10.1021/pr900699a>.
- Upadhyaya R, Kim K, Hogue-Angeletti R, Weiss LM. 2011. Improved techniques for endogenous epitope tagging and gene deletion in *Toxoplasma gondii*. *J Microbiol Methods* 85:103–113. <http://dx.doi.org/10.1016/j.mimet.2011.02.001>.
- Roiko MS, Carruthers VB. 2009. New roles for perforins and proteases in apicomplexan egress. *Cell Microbiol* 11:1444–1452. <http://dx.doi.org/10.1111/j.1462-5822.2009.01357.x>.
- Nardelli SC, Che FY, Silmon de Monerri NC, Xiao H, Nieves E, Madrid-Aliste C, Angel SO, Sullivan WJ, Jr, Angeletti RH, Kim K, Weiss LM. 2013. The histone code of *Toxoplasma gondii* comprises conserved and unique posttranslational modifications. *mBio* 4:e00922-00913. <http://dx.doi.org/10.1128/mBio.00922-13>.
- Brooks CF, Francia ME, Gissot M, Croken MM, Kim K, Striepen B. 2011. *Toxoplasma gondii* sequesters centromeres to a specific nuclear region throughout the cell cycle. *Proc Natl Acad Sci U S A* 108:3767–3772. <http://dx.doi.org/10.1073/pnas.1006741108>.
- Hu K. 2008. Organizational changes of the daughter basal complex during the parasite replication of *Toxoplasma gondii*. *PLoS Pathog* 4:e10. <http://dx.doi.org/10.1371/journal.ppat.0040010>.
- Mann T, Beckers C. 2001. Characterization of the subpellicular network, a filamentous membrane skeletal component in the parasite *Toxoplasma gondii*. *Mol Biochem Parasitol* 115:257–268. [http://dx.doi.org/10.1016/S0166-6851\(01\)00289-4](http://dx.doi.org/10.1016/S0166-6851(01)00289-4).
- Gubbels MJ, Vaishnava S, Boot N, Dubremetz JF, Striepen B. 2006. A MORN-repeat protein is a dynamic component of the *Toxoplasma gondii* cell division apparatus. *J Cell Sci* 119:2236–2245. <http://dx.doi.org/10.1242/jcs.02949>.
- Beck JR, Rodriguez-Fernandez IA, de Leon JC, Huynh MH, Carruthers VB, Morrisette NS, Bradley PJ. 2010. A novel family of *Toxoplasma* IMC proteins displays a hierarchical organization and functions in coordinating parasite division. *PLoS Pathog* 6:e1001094. <http://dx.doi.org/10.1371/journal.ppat.1001094>.
- Suvorova ES, Francia M, Striepen B, White MW. 2015. A novel bipartite centrosome coordinates the apicomplexan cell cycle. *PLoS Biol* 13: e1002093. <http://dx.doi.org/10.1371/journal.pbio.1002093>.
- Bahl A, Davis PH, Behnke M, Dzierszinski F, Jagalur M, Chen F, Shanmugam D, White MW, Kulp D, Roos DS. 2010. A novel multifunctional oligonucleotide microarray for *Toxoplasma gondii*. *BMC Genomics* 11:603. <http://dx.doi.org/10.1186/1471-2164-11-603>.
- Croken MM, Qiu W, White MW, Kim K. 2014. Gene set enrichment analysis (GSEA) of *Toxoplasma gondii* expression datasets links cell cycle progression and the bradyzoite developmental program. *BMC Genomics* 15:515. <http://dx.doi.org/10.1186/1471-2164-15-515>.

21. Francia ME, Jordan CN, Patel JD, Sheiner L, Demerly JL, Fellows JD, de Leon JC, Morrisette NS, Dubremetz JF, Striepen B. 2012. Cell division in apicomplexan parasites is organized by a homolog of the striated rootlet fiber of algal flagella. *PLoS Biol* 10:e1001444. <http://dx.doi.org/10.1371/journal.pbio.1001444>.
22. Bachand F. 2007. Protein arginine methyltransferases: from unicellular eukaryotes to humans. *Eukaryot Cell* 6:889–898. <http://dx.doi.org/10.1128/EC.00099-07>.
23. Pahllich S, Zakaryan RP, Gehring H. 2006. Protein arginine methylation: cellular functions and methods of analysis. *Biochim Biophys Acta* 1764: 1890–1903. <http://dx.doi.org/10.1016/j.bbapap.2006.08.008>.
24. Gary JD, Lin WJ, Yang MC, Herschman HR, Clarke S. 1996. The predominant protein-arginine methyltransferase from *Saccharomyces cerevisiae*. *J Biol Chem* 271:12585–12594. <http://dx.doi.org/10.1074/jbc.271.21.12585>.
25. Pelletier M, Pasternack DA, Read LK. 2005. In vitro and in vivo analysis of the major type I protein arginine methyltransferase from *Trypanosoma brucei*. *Mol Biochem Parasitol* 144:206–217. <http://dx.doi.org/10.1016/j.molbiopara.2005.08.015>.
26. Pawlak MR, Scherer CA, Chen J, Roshon MJ, Ruley HE. 2000. Arginine N-methyltransferase 1 is required for early postimplantation mouse development, but cells deficient in the enzyme are viable. *Mol Cell Biol* 20:4859–4869. <http://dx.doi.org/10.1128/MCB.20.13.4859-4869.2000>.
27. Bachand F, Silver PA. 2004. PRMT3 is a ribosomal protein methyltransferase that affects the cellular levels of ribosomal subunits. *EMBO J* 23: 2641–2650. <http://dx.doi.org/10.1038/sj.emboj.7600265>.
28. Ghaemmaghami S, Huh WK, Bower K, Howson RW, Belle A, Dephoure N, O'Shea EK, Weissman JS. 2003. Global analysis of protein expression in yeast. *Nature* 425:737–741. <http://dx.doi.org/10.1038/nature02046>.
29. Tang J, Gary JD, Clarke S, Herschman HR. 1998. PRMT 3, a type I protein arginine N-methyltransferase that differs from PRMT1 in its oligomerization, subcellular localization, substrate specificity, and regulation. *J Biol Chem* 273:16935–16945. <http://dx.doi.org/10.1074/jbc.273.27.16935>.
30. Henry MF, Silver PA. 1996. A novel methyltransferase (Hmt1p) modifies poly(A)+-RNA-binding proteins. *Mol Cell Biol* 16:3668–3678. <http://dx.doi.org/10.1128/MCB.16.7.3668>.
31. Subramaniam C, Veazey P, Redmond S, Hayes-Sinclair J, Chambers E, Carrington M, Gull K, Matthews K, Horn D, Field MC. 2006. Chromosome-wide analysis of gene function by RNA interference in the African trypanosome. *Eukaryot Cell* 5:1539–1549. <http://dx.doi.org/10.1128/EC.00141-06>.
32. Fisk JC, Read LK. 2011. Protein arginine methylation in parasitic protozoa. *Eukaryot Cell* 10:1013–1022. <http://dx.doi.org/10.1128/EC.05103-11>.
33. Behnke MS, Wootton JC, Lehmann MM, Radke JB, Lucas O, Nawas J, Sibley LD, White MW. 2010. Coordinated progression through two sub-transcriptomes underlies the tachyzoite cycle of *Toxoplasma gondii*. *PLoS One* 5:e12354. <http://dx.doi.org/10.1371/journal.pone.0012354>.
34. Dhar S, Vemulapalli V, Patananan AN, Huang GL, Di Lorenzo A, Richard S, Comb MJ, Guo A, Clarke SG, Bedford MT. 2013. Loss of the major type I arginine methyltransferase PRMT1 causes substrate scavenging by other PRMTs. *Sci Rep* 3:1311. <http://dx.doi.org/10.1038/srep01311>.
35. Braun L, Cannella D, Ortet P, Barakat M, Sautel CF, Kieffer S, Garin J, Bastien O, Voinnet O, Hakimi MA. 2010. A complex small RNA repertoire is generated by a plant/fungal-like machinery and effected by a metazoan-like Argonaute in the single-cell human parasite *Toxoplasma gondii*. *PLoS Pathog* 6:e1000920. <http://dx.doi.org/10.1371/journal.ppat.1000920>.
36. Kirino Y, Kim N, de Planell-Saguer M, Khandros E, Chiorean S, Klein PS, Rigoutsos I, Jongens TA, Mourelatos Z. 2009. Arginine methylation of piwi proteins catalysed by dPRMT5 is required for Ago3 and Aub stability. *Nat Cell Biol* 11:652–658. <http://dx.doi.org/10.1038/ncb1872>.
37. Musiyenko A, Majumdar T, Andrews J, Adams B, Barik S. 2012. PRMT1 methylates the single Argonaute of *Toxoplasma gondii* and is important for the recruitment of Tudor nuclease for target RNA cleavage by antisense guide RNA. *Cell Microbiol* 14:882–901. <http://dx.doi.org/10.1111/j.1462-5822.2012.01763.x>.
38. Heaslip AT, Dziarszynski F, Stein B, Hu K. 2010. TgMORN1 is a key organizer for the basal complex of *Toxoplasma gondii*. *PLoS Pathog* 6:e1000754. <http://dx.doi.org/10.1371/journal.ppat.1000754>.
39. Lorestani A, Sheiner L, Yang K, Robertson SD, Sahoo N, Brooks CF, Ferguson DJ, Striepen B, Gubbels MJ. 2010. A *Toxoplasma* MORN1 null mutant undergoes repeated divisions but is defective in basal assembly, apicoplast division and cytokinesis. *PLoS One* 5:e12302. <http://dx.doi.org/10.1371/journal.pone.0012302>.
40. Chen CT, Gubbels MJ. 2013. The *Toxoplasma gondii* centrosome is the platform for internal daughter budding as revealed by a Nek1 kinase mutant. *J Cell Sci* 126:3344–3355. <http://dx.doi.org/10.1242/jcs.123364>.
41. Zhou Z, Sun X, Zou Z, Sun L, Zhang T, Guo S, Wen Y, Liu L, Wang Y, Qin J, Li L, Gong W, Bao S. 2010. PRMT5 regulates Golgi apparatus structure through methylation of the golgin GM130. *Cell Res* 20: 1023–1033. <http://dx.doi.org/10.1038/cr.2010.56>.
42. Karkhanis V, Hu YJ, Baiocchi RA, Imbalzano AN, Sif S. 2011. Versatility of PRMT5-induced methylation in growth control and development. *Trends Biochem Sci* 36:633–641. <http://dx.doi.org/10.1016/j.tibs.2011.09.001>.
43. Fisk JC, Li J, Wang H, Aletta JM, Qu J, Read LK. 2013. Proteomic analysis reveals diverse classes of arginine methylproteins in mitochondria of trypanosomes. *Mol Cell Proteomics* 12:302–311. <http://dx.doi.org/10.1074/mcp.M112.022533>.
44. Lott K, Li J, Fisk JC, Wang H, Aletta JM, Qu J, Read LK. 2013. Global proteomic analysis in trypanosomes reveals unique proteins and conserved cellular processes impacted by arginine methylation. *J Proteomics* 91:210–225. <http://dx.doi.org/10.1016/j.jprot.2013.07.010>.
45. Fan Q, Miao J, Cui L, Cui L. 2009. Characterization of PRMT1 from *Plasmodium falciparum*. *Biochem J* 421:107–118. <http://dx.doi.org/10.1042/BJ20090185>.
46. Donald RG, Roos DS. 1998. Gene knockouts and allelic replacements in *Toxoplasma gondii*: HXGPRT as a selectable marker for hit-and-run mutagenesis. *Mol Biochem Parasitol* 91:295–305. [http://dx.doi.org/10.1016/S0166-6851\(97\)00210-7](http://dx.doi.org/10.1016/S0166-6851(97)00210-7).
47. Ponting CP. 1999. Chlamydial homologues of the MACPF (MAC/perforin) domain. *Curr Biol* 9:R911–R913. [http://dx.doi.org/10.1016/S0960-9822\(00\)80102-5](http://dx.doi.org/10.1016/S0960-9822(00)80102-5).
48. Pfefferkorn ER, Pfefferkorn LC. 1977. Specific labeling of intracellular *Toxoplasma gondii* with uracil. *J Protozool* 24:449–453. <http://dx.doi.org/10.1111/j.1550-7408.1977.tb04774.x>.
49. Håkansson S, Morisaki H, Heuser J, Sibley LD. 1999. Time-lapse video microscopy of gliding motility in *Toxoplasma gondii* reveals a novel, bi-phasic mechanism of cell locomotion. *Mol Biol Cell* 10:3539–3547. <http://dx.doi.org/10.1091/mbc.10.11.3539>.
50. Lagal V, Binder EM, Huynh MH, Kafsack BF, Harris PK, Diez R, Chen D, Cole RN, Carruthers VB, Kim K. 2010. *Toxoplasma gondii* protease TgSUB1 is required for cell surface processing of micronemal adhesive complexes and efficient adhesion of tachyzoites. *Cell Microbiol* 12: 1792–1808. <http://dx.doi.org/10.1111/j.1462-5822.2010.01509.x>.
51. Suvorova ES, Lehmann MM, Kratzer S, White MW. 2012. Nuclear action-related protein is required for chromosome segregation in *Toxoplasma gondii*. *Mol Biochem Parasitol* 181:7–16. <http://dx.doi.org/10.1016/j.molbiopara.2011.09.006>.
52. Shechter D, Dormann HL, Allis CD, Hake SB. 2007. Extraction, purification and analysis of histones. *Nat Protoc* 2:1445–1457. <http://dx.doi.org/10.1038/nprot.2007.202>.
53. Madrid-Aliste CJ, Dybas JM, Angeletti RH, Weiss LM, Kim K, Simon I, Fiser A. 2009. EPIC-DB: a proteomics database for studying apicomplexan organisms. *BMC Genomics* 10:38. <http://dx.doi.org/10.1186/1471-2164-10-38>.
54. Behnke MS, Radke JB, Smith AT, Sullivan WJ, Jr, White MW. 2008. The transcription of bradyzoite genes in *Toxoplasma gondii* is controlled by autonomous promoter elements. *Mol Microbiol* 68:1502–1518. <http://dx.doi.org/10.1111/j.1365-2958.2008.06249.x>.